Ultra-High Surface Area Activated Carbon from Bacterial Cellulose via Potassium Carbonate Catalyzed Pyrolysis: Mechanisms and Applications

Hamideh Najarzadeh[1], Abosaeed Rashidi[1]*, Ramin Khajavi[2,3], Mohammad Esmail Yazdanshenas[1], Amin Meftahi[2,3]

[1] Department of Textile Engineering, SR.C., Islamic Azad University, Tehran, Iran.

[2]Department of Chemical & Polymer Engineering, ST.C, Islamic Azad University, Tehran, Iran.

[3]Nanotechnology Research Center, ST.C, Islamic Azad University, Tehran,Iran.

*Corresponding author, Email: Rashidi@srbiau.ac.ir , rashidi50@yahoo.com

Abstract

This study aimed to enhance the production of high-quality activated carbon (AC) from bacterial cellulose (BC) through a strategic potassium carbonate (PC) pretreatment. We meticulously evaluated the properties of activated carbon derived from unmodified bacterial cellulose (ACUM) and compared them with those obtained from PC-modified bacterial cellulose (ACM), unequivocally demonstrating the profound success of this chemical pretreatment methodology.

The results were striking: compared to ACUM, the PC-modified BC (ACM) exhibited a remarkable increase in carbon content, reaching 85.43% from an initial 65.16%. Furthermore, its pore volume surged to an impressive 0.844 cm^3/g, significantly higher than ACUM's 0.339 cm^3/g. Most notably, the specific surface area of ACM dramatically doubled, achieving 1600.14 m^2/g compared to ACUM's 800.94 m^2/g.

In-depth mechanistic studies provided crucial insights, revealing that PC actively promotes the formation of a more homogeneous pore structure within the carbon material. Concurrently, it effectively reduces the pyrolysis temperatures required for efficient carbonization of the bacterial cellulose. This groundbreaking work significantly advances the design and development of sustainable, high-performance AC, opening new avenues for its application in critical areas such as environmental remediation and a diverse array of biomedical applications.

Keywords: Activated carbon (AC) - bacterial cellulose (BC) - potassium carbonate (PC) - activated carbon from unmodified bacterial cellulose (ACUM) - activated carbon from modified bacterial cellulose (ACM).

1. Introduction

Activated carbon (AC) is an efficient adsorbent for various industrial purposes. The highly adsorbent surface owes its functionality to a high specific surface area, developed porous structure, and high surface activity (surface energy) [1]. Activated carbon is used as an adsorbent in various industries for various purposes, such as purification [2], disinfection [3], decolorization [4], separation [5], and condensation [6,7]. The highly functional material has proven useful in different industries and applications such as food [8], pharmaceutical [9], petroleum [10], gas [11], petrochemical [12], nuclear power [13], medicine [14], automotive [15], dyes and resins [16], drinking water treatment [17] and industrial effluents [18].

The source of the raw material used to make activated carbon has an impact on the final adsorption quality [19]. It is possible to produce AC as a raw material from any substance that is rich in carbon and has just a tiny quantity of minerals and volatiles. Evidently, the use of cheaper sources for AC production results in a low-cost product that can be vastly applied. Therefore, agricultural wastes are the most suitable raw materials to produce activated carbon in terms of their properties as well as their cheapness and abundance [20]. These include walnut shell [21], almond shell [22], hazelnut shell [23], coconut shell [24], olive seed [25], grape seed [26], sugarcane pulp [27] and rice husk [28]. Although utilized for specific purposes and in limited applications, in addition to agricultural wastes, other polymers and mineral materials, such as worn tires [29], newspaper waste [30], palm trees [31], and coal [32] have been used to produce activated carbon. Among the different biopolymers, since bacterial cellulose (BC) is highly pure and has a microfibrillar structure and a high specific surface area with a low production cost, it is expected that the produced AC have a particular specific surface area and unique properties [33-34].

BC produced by *Acetobacter xylinum*, which has attracted the attention of many researchers in recent years, is a renewable material with very desirable properties. *Acetobacter xylinum* is a non-photosynthetic organism that can convert carbon sources, such as glucose, sugar, and glycerol into pure nanocellulose [35]. Due to high adsorption, crystallization, high water retention, tensile strength, and resistance to organic solvents, several industries have benefited from using BC [36]. Additionally, BC has attracted the attention of many researchers due to its unique properties, such as interesting mechanical properties in both dry and wet states, porosity, water absorption, ductility, biodegradability, and biocompatibility [37]. The fiber size of about 100 times smaller than plant cellulose is considered an additional advantage, which enables the nano-sized material to have a

high water holding capacity (more than 200 times the dry weight), elasticity, wet strength, and adaptability. Moreover, due to the small size of BC fibers, this product is used in wound healing and vascular implants [38]. The highly nano-porous substance that allows antibiotics or other drugs to enter the wound, while simultaneously protecting the site from infection from the outside [39].

Owing to the unique properties of BC, the production of activated carbon from this cellulose source is considered an important revolution in various industries [40]. Accordingly, it is expected that AC produced from BC, in addition to improving the properties of bacterial cellulose, can have various applications in different industries, especially medical and healthcare with regards to its safety and compatibility with the human body.

So far, few studies have focused on the production of AC from bacterial cellulose. In 2013, *Long Lee et al.* used the activated carbon-produced BC to improve energy storage in electrical capacitors and use it to produce superconductors. The researchers used BC extracted from *Nata-de-Coco* as a source for the production of activated carbon at the nanoscale in bilayer capacitors [41].

Furthermore, in 2019, *Arnon Khamkeawa et al.* conducted a study in which AC produced from bacterial cellulose was used as a catalyst to convert ethanol to ethylene. They showed that the adsorption level of activated carbon produced from bacterial cellulose changes by using different percentages of H_3PO_4 [42]. In the same year, this group of researchers conducted another study on activated carbon derived from BC, using it as an adsorbent to remove dyes from an aqueous solution [43].

In 2022, the production of activated carbon from BC for the synthesis of a meso-porous catalyst and the function of the catalyst in bioethanol dehydration were studied. The highly regular structure of this catalyst for mass transfer leads to improved conversion and selectivity as well as reduced coke deposits [44].

Due to the importance of harshness reduction of activation cellulose treatment, we introduced a modified method, in which carbon activation was achieved through chemical pretreatment of BC using PC. In addition of being environmentally friendly, the requisite activation rate can be obtained with a lower concentration and convert them to AC through the method. Moreover, the effect of modification on the physical and chemical characteristics of obtained activated carbon (ACM) was investigated [45].

2. Materials and Methods

2.1 Materials

Acetobacter xylinum (AATCC 23768) was used for BC synthesis. The combination of 2.0% D-glucose, 0.5% peptone, 0.5% yeast extract, 0.115% citric acid, and 0.27% disodium hydrogen phosphate was mixed with distilled water for preparing Hestrin-Schramm (HS) culture medium. The BC pellicles were collected after a 10-day cultivation period from the surface of a static culture medium. The BC pellicles were purified in boiling water containing 0.1 N NaOH solution for 90 min, followed by neutralizing and rinsing in distilled water. In the following step, K_2Co_3 (potassium carbonate, Sigma Aldrich Company, USA) was applied to chemically activate BC [46].

2.2 Methods

2.2.1 Preparation of Activated Carbon

After BC purification, PC solution (0.01%, w/v) was used as a chemical modifier, and then samples were fully dried at room temperature for 48h. The activation process was completed by heat exposure at 110°C for 24 hours. In the last step of activation, the samples were incubated in the oven at 500 °C for 1 hour, and then, a solution of 1% HCl (mol / dm^3) and distilled water was used to wash the samples for 4 hours at 70 °C (120 rpm) to reach pH=7 [53].

2.2.2. Characterization of Activated Carbon

X-ray diffraction (XRD) (SIEMENS D5000 X-ray diffractometer, Aubrey, USA) was applied to determine the bulk crystal structure of AC using CuKα radiation with Ni filter in the 2θ range of 10°–80° with a resolution of 0.04°. Fourier Transform Infrared (FT-IR) spectroscopy (Nicolet 6700 FTIR spectrometer, Thermo Scientific, USA) was applied to identify the chemical structure of samples. The surface area, pore volume, and pore diameter of AC were determined by nitrogen (N2) physisorption–desorption at a liquid N_2 temperature of −196 °C using a Micromeritics Chemisorb 2750 Pulse instrument (Norcross, GA, USA). Field Emission Scanning Electron Microscope and Energy Dispersive X-Ray (FESEM-EDX) Spectrometer (Model of JSM7610F and X-MaxN 20, JEOL, USA) were used to observe the morphology of AC and the presence of existing elements. To investigate the thermal analysis of the samples, Thermal Gravimetric Analysis (TGAQ600, USA) was used. To study the pore volume, surface area, porosity, and the structure of the pores BET/BJH (BEL-type Belsorp mini II, Japan) was applied.

3. Results and Discussion

Applying K_2CO_3 as alkaline material decreases BC pyrolysis temperature and enhances carbonization [47]. PC initiates the pyrolysis process at a lower temperature, increases the degradation of hydrogen bonds and improves glycosidic linkage in the cellulose chemical structure, which changes the BC to the levoglucosan. Levoglucosan is an intermediate material in the process of cellulose burning. Ultimately, BC heat exposure results in biochar produced through pyrolysis [48]. PC could introduce a new path to cellulose decomposition and provide a more porous AC structure from BC with improved pore volume size and different shapes. When the BC was soaked in an alkaline solution, the ion migration kinetics result in more homogenous pores and enhances specific surface area [49].

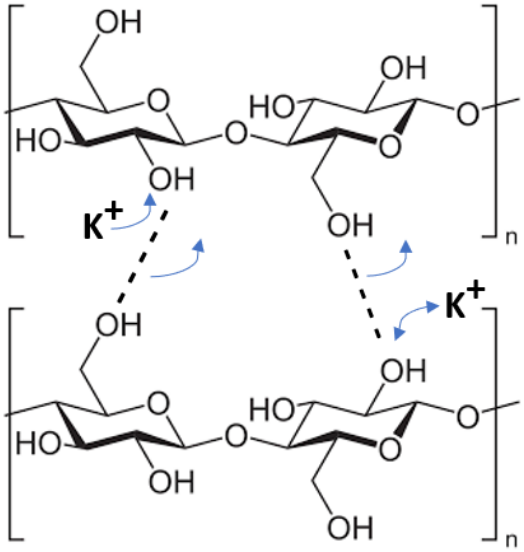

Fig. 1 Shows the mechanism of cellulose pyrolysis in the presence of K_2CO_3[50]

3.1 Field Emission Scanning Electron Microscope (FESEM)

FESEM, a high-magnification microscopic technique, was used to study the physical and morphological structure of the samples, in scales of 20 μm, 1μm, and 200nm, in order to observe the surface of ACs. As shown in Fig 2, the ACM (C and D) was more porous compared to ACUM (A and B), which indicates that activation has led to an increase in the number of pores and pore shape differences in ACM and ACUM. According to Fig 2, the size of the ACUM pores was smaller than the ACM, which is related to the K_2CO_3 and the activation process. The hole shapes of both samples are cave-like but the ACUM holes are inhomogeneous compared to ACM. The migration of ions in the activation process causes uniform porosity in ACM samples[51]. During the

production of AC, bacterial cellulose was exposed to heat and this leads to the formation of bitumen as BC melts. The presence of these structures reduces the number of pores and, consequently, the adsorption of activated carbon [52]. Therefore, the use of an activating substance in the production process leads to the pores being filled with the activation substance. Following the production of activated carbon and the completion of the process, the activation substance comes out of the pores in the washing step, resulting in the maintenance of pores and an increase in the adsorption rate [53]. The diameter of the pores shows more uniformity compared to ACUM. Moreover, the activation process has accelerated carbonization in BC and enhanced the degradation of samples. The surface area in ACM is higher than ACUM. This phenomenon increases the absorption of the treated samples, making these structures more appropriate for medical purposes [54].

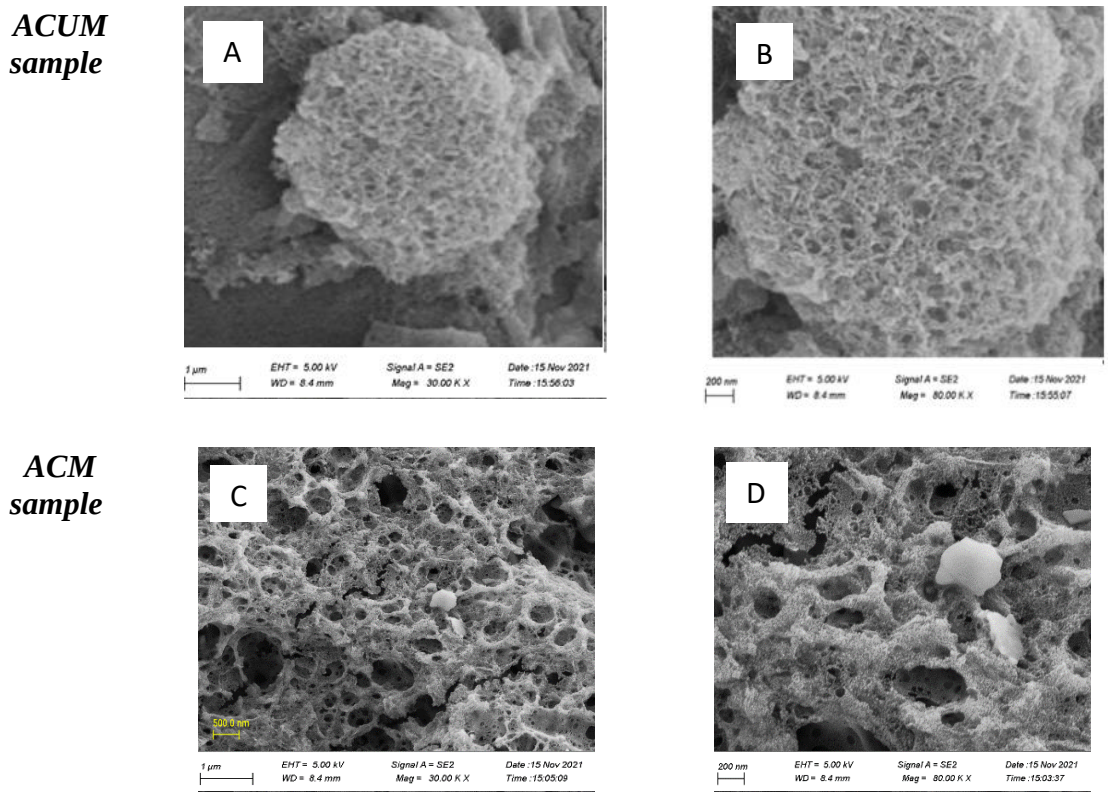

Fig. 2 Field Emission Scanning Electron Microscopy of (A and B) ACUM sample (C and D) ACM sample

3.2. X-ray diffraction spectrometer (XRD)

XRD or X-ray diffraction is a non-destructive method of structural analysis which reports comprehensive and useful information about the crystal structure of materials. Each crystal structure has its characteristic X-ray pattern which can be used as a fingerprint for identification. XRD analysis allows the preparation of material diffraction patterns and studying properties such as qualitative determination of unknown crystalline compounds, determining unique phase, size and orientation of crystals, stresses, and lattice defects [55].

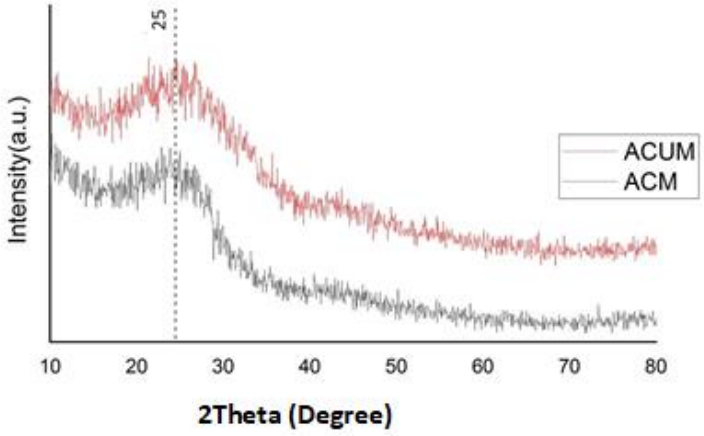

Fig. 3 XRD pattern of ACUM and ACM samples

The XRD patterns of ACM and ACUM carbonized BC are illustrated in Fig 3. Typical peak of activated carbon is observed around 25°. XRD patterns of activated and not activated samples show similarity between the ACM and ACUM graphs, which is related to the structure of amorphous carbon composed of aromatic carbon sheets [61].

3.3. Fourier Transform Infrared Spectroscopy (FTIR)

FTIR test is performed to examine the functional groups and the chemical bonds which are formed due to chemical reactions. Functional groups of ACUM and ACM were identified in the wavelength range of 500 to 4000 cm^{-1}.

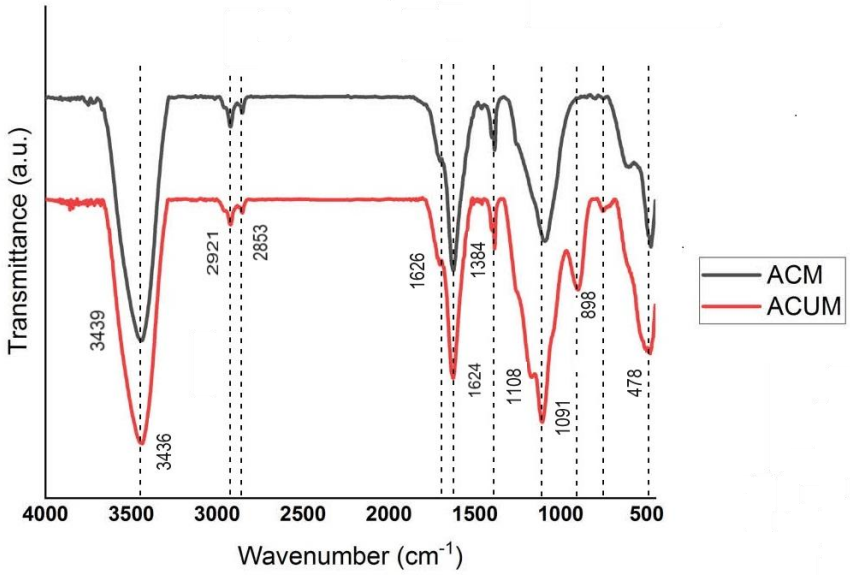

Fig. 4 FTIR spectra of ACUM and ACM sample

The absorption peak at 3436 cm^{-1} is related to the presence of a hydroxyl group in the chemical structure of BC. The symmetrical tensile vibration of the C-H causes the peak at the wavelength of 2921cm^{-1}, which indicates the presence of carbon in the system and BC carbonization. This peak can also be the result of interactions with the carbon present on the surface. The peak at 1626 cm^{-1} can either be due to carbonization or the formation of a double bond between carbon atoms. The peaks can also be observed at the following wavelengths: 1384 cm-^{1}, related to CH_2-CH_3 bending vibrations, 1108 cm^{-1} and 898 cm^{-1}, related to BC C-O tensile vibration, 478 cm^{-1}, related to existing pollutants, 3439 cm^{-1} due to the presence of moisture and OH bond vibration, 2921 cm^{-1} and 2853 cm^{-1}, the result of CH tensile vibration in both the BC and the modifier, 1624 cm^{-1} the result of carbonization and formation of a double bond between carbon atoms, 1384 cm^{-1}, related to CH_2-CH_3 and carbonate vibration, and 1091 cm^{-1} as a result of CO tensile vibration in BC and carbonate [55,56,57].

The higher peaks from 1000 to 1100 cm^{-1} are due to the abundance of oxygen in ACUM, which means the scarcity of carbon. While in the absence of activator, the higher amounts of oxygen lead to an increase in the distance of the plates and layers, its presence results in more intense peaks in 1600 to 3000 cm^{-1}, the indication of lower C-O bonds [43]. Moreover, the 475 cm^{-1} peak is the result of pollutants and the comb-shaped peak at 700 cm^{-1} is the result of the bending vibration of internal and external elements in plates [58].

3.4 Energy Dispersive X-ray (EDX)

EDX testing examines the chemical composition of microstructures to determine the different phases of a substance and plays an important role in the recognition and identification of unknown phases. EDX is used for structural analysis and element analysis of the samples. As shown in Table 1, the ACM sample, activated using PC, possesses half the amount of oxygen in comparison with the inactivated sample, while its carbon percentage is nearly twice compared to the inactivated form. It means that the presence of K_2Co_3 facilitates the pyrolysis of BC through the melting process and inside penetration of ACM. Therefore, more carbon element increases the amount of AC in the ACM sample compared to the ACUM sample [56,59]. In addition, the decrease in the amount of oxygen also demonstrated that the activated BC showed more potential for carbonization.

Table 1 EDX result of ACUM and ACM samples

Sample	**C** (Weight %)	**O** (Weight %)	**Other** (Weight %)
ACUM	65.16	27.11	7.73
ACM	85.43	13.64	0.93

3.5 Thermogravimetric Analysis (TGA)

TGA is a method of thermal analysis in which the mass of a sample is measured over time as the temperature changes. This measurement provides information about physical phenomena, such as phase transitions, absorption, adsorption and desorption. This test was performed in the temperature range from ambient temperature to 1000°C and a heating rate of 10°C /min and in a nitrogen medium between activated and inactivated samples [60].

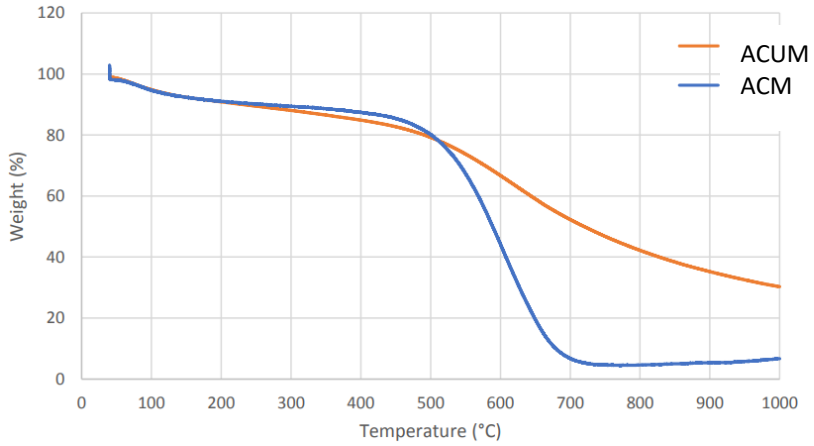

Fig. 5 TGA test of ACUM and ACM samples

As shown in Fig.5, there are two major weight losses in ACUM. The first weight loss happens in a temperature below 200$^{\circ C}$ and the second in temperatures ranging from 400 to 500$^{\circ C}$. At temperatures below 200$^{\circ C}$, weight loss is due to water loss, namely evaporation of moisture inside the samples. Weight loss in the range of 400 to 500$^{\circ C}$ starts from 360$^{\circ C}$ due to the loss of cellulose in the samples. When the inactivated sample is exposed to heat, first, parts of the activated carbon is melted, leading to the formation of bitumen and filling the pores. Therefore, as the pores are closed, followed by the exposure to heat, the surface burns and prevents the rest of the parts from burning completely. This prevents pore destruction and leads to higher adsorption in AC [55].

Similarly, there are two major weight losses in ACM. The first weight loss is observed in temperatures below 200$^{\circ C}$ and the second has happened in the temperatures of 400 to 650$^{\circ C}$. At temperatures below 200$^{\circ C}$, minor weight loss is reported due to water evaporation of moisture and the low slope of the diagram indicates the low weight percentage of this part of the material (i.e. there is little moisture in the sample). Weight loss in the temperatures ranging from 400 to 650$^{\circ C}$ has started from 320$^{\circ C}$ due to the loss of cellulose in the samples. The significant point is that, as can be seen, the activation material fills the activated carbon pores while the activation agent is present in the samples, and it is washed out of the pores after the washing step. Therefore, the internal structure of the activated carbon is more accessible to the heat resulting in its faster penetration into the activated carbon. However, major weight loss is experienced as the slope of the diagram falls sharply in these temperatures [56].

3.6 BET- BJH

BET and BJH methods are fast and relatively low-cost for statistical analysis of surface size, mean particle size, porosity, porosity shape and size of micro, meso and macro. In this paper, these methods were used to measure the diameter of activated carbon cavities.

Table 2 Specific surface area, cavity volume and mean pore diameters for activated (ACM) and inactivated (ACUM) samples

	$a_{s, BET}$ (m^2 /g)	Total pore volume(p/p_0=0.990) (cm^3/g)	Mean pore diameter (nm)

ACUM	800.94	0.339	6.65
ACM	1600.14	0.844	5.89

Nitrogen gas adsorption and desorption were applied in the investigation of the specific surface area, volume, and size of cavities. The impact of different factors, such as activation, was also examined. The comparison of the properties of activated (ACM) and inactivated (ACUM) carbon are illustrated in Table 2. Compared to the inactivated sample, a significant increase in specific surface area is generally observed due to activation. The BET conducted on ACUM and ACM reported the specific surface area of the samples 800.94 and 1600.14 (m^2/g), respectively. As a result of activation, the diameter of cavities has doubled as the increase in surface area is experienced. The isothermal shape of both samples falls under IV type in the IUPAC classification, an indication of mesoporosity and their conical shapes [48] (Fig 6). Applying PC, as the activating agent, to bacterial cellulose can be an important and effective step in the production of activated carbon with unique properties. A comparison of the activated carbon produced in this study with other previous studies [56] can confirm this.

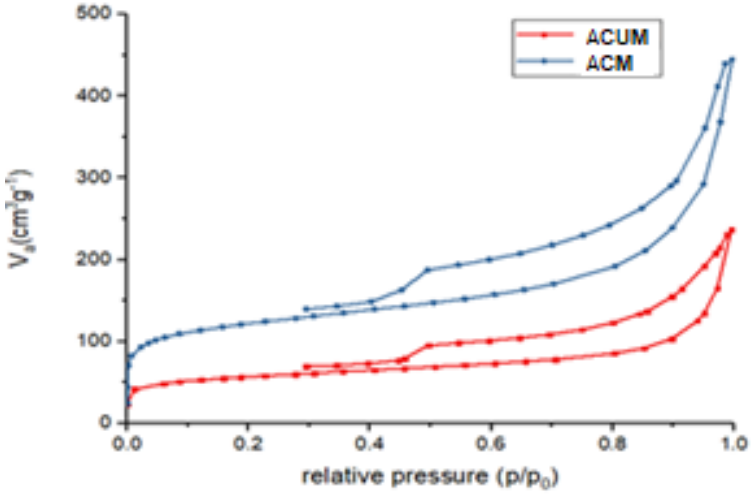

Fig. 6 Nitrogen adsorption-desorption isotherm for inactivated (ACUM) and activated (ACM) bacterial cellulose

Conclusion

Bacterial cellulose (BC) produced by Acetobacter xylinum has received much attention in recent years as a renewable material with desirable properties. Acetobacter xylinum is a non-photosynthetic organism that can convert sources of carbon, such as glucose, sugar and glycerol, into pure nanocellulose. BC has the same chemical structure as plant cellulose, but has a uniform nanofiber network structure and unique properties including high crystallinity, porosity and surface area for adsorption, water-holding capacity, tensile strength, and resistance to organic solvents.

BC has been used in a wide range of applications, including raw material in food industries, a reinforcing agent for paper and biocompatible material for biomedical applications. Due to its advantageous properties, BC has great potential to be used as source material for highly efficient activated carbon (AC) adsorbents. Characterization and evaluation of AC adsorbents derived from BC have proven their functionality. Generally, AC is produced by either a physical or chemical process. The physical activation process involves two steps, carbonization and activation, both of which are conducted at high temperatures. Chemical activation has advantages over physical activation. The required temperature is lower, it produces a higher yield of AC with a higher surface area and usually involves only one step.

The PC pretreatment strategy transforms bacterial cellulose into high-performance activated carbon (ACM) with unprecedented carbon content (85.43%) and surface area (1600.14 m^2/g), outperforming conventional methods (ACUM). The key role of PC in lowering pyrolysis temperatures and creating uniform mesopores was validated through SEM, BET, and TGA analyses. These advances position ACM as a sustainable alternative for environmental applications and biomedical uses.

Data availability

The datasets generated and analyzed during this study are available from the corresponding author upon reasonable request.

Declarations

Conflict of interest

The authors declare that they have no known competing financial interests or personal relationships that could have appeared to influence the work reported in this paper.

Ethical approval

Not applicable. This research did not involve human participants, animals, or any data requiring ethical approval

References

1. Dias JM, Alvim-Ferraz MC, Almeida MF, Rivera-Utrilla J, & Sánchez-Polo M (2007) Waste materials for activated carbon preparation and its use in aqueous-phase treatment: a review. J Environ Manage 85(4), 833-846. https://doi.org/10.1016/j.jenvman.2007.07.031.

2. Durán I, Álvarez-Gutiérrez N, Rubiera F, & Pevida CJCEJ (2018) Biogas purification by means otsf adsorption on pine sawdust-based activated carbon: Impact of water vapor. Chem. Eng J 353, 197-207. https://doi.org/10.1016/j.cej.2018.07.100.

3. Chen L, Pinto A, & Alshawabkeh A N (2019) Activated carbon as a cathode for water disinfection through the electro-fenton process. Focus Catal Focus on 9(7), 601-606. https://doi.org/10.3390/catal9070601.

4. Rahimian R, & Zarinabadi S (2020) A review of studies on the removal of methylene blue dye from industrial wastewater using activated carbon adsorbents made from almond bark. Prog Chem Biochem Res 3(3), 251-268. https://doi.org/10.33945/SAMI/PCBR.2020.3.8.

5. Nejadshafiee V, & Islami MR (2019) Adsorption capacity of heavy metal ions using sultone-modified magnetic activated carbon as a bio-adsorbent. Mater Sci Eng, C 101, 42-52. https://doi.org/10.1016/j.msec.2019.03.081.

6. Heidarinejad Z, Dehghani MH, Heidari M, Javedan G, Ali I, & Sillanpää M (2020) Methods for preparation and activation of activated carbon: a review. Environ Chem Lett 18(2), 393-415. https://doi.org/10.1007/s10311-019-00955-0.

7. Winter C, Caetano JN, Araújo ABC, Chaves AR, Ostroski IC, Vaz BG, & Alonso CG (2016) Activated carbons for chalcone production: Claisen-Schmidt condensation reaction. Chem Eng J 303, 604-610. https://doi.org/10.1016/j.cej.2016.06.058.

8. Purnawati AS (2021) Treatment of Salt for Food-Grade Using Activated Carbon. Adv Mater Res (Vol. 1162, pp. 9-14). Trans Tech Publications Ltd, 9-14. https://doi.org/10.4028/www.scientific.net/AMR.1162.9.

9. Mansour F, Al-Hindi M, Yahfoufi R, Ayoub GM, & Ahmad MN (2018) The use of activated carbon for the removal of pharmaceuticals from aqueous solutions: a review. Rev Environ Sci Bio/Technol 17(1), 109-145. https://doi.org/10.1007/s11157-017-9456-8.

10. Ani JU, Akpomie KG, Okoro UC, Aneke LE, Onukwuli OD, & Ujam OT (2020) Potentials of activated carbon produced from biomass materials for sequestration of dyes, heavy metals, and crude oil components from aqueous environment. Appl Water Sci 10(2), 1-11. https://doi.org/10.1007/s13201-020-1149-8.

11. Pallarés J, González-Cencerrado A, & Arauzo I (2018) Production and characterization of activated carbon from barley straw by physical activation with carbon dioxide and steam. Biomass Bioenergy 115, 64-73. https://doi.org/10.1016/j.biombioe.2018.04.015.

12. Hu J, Fu W, Ni F, Zhang X, Yang C, & Sang J (2020) An integrated process for the advanced treatment of hypersaline petrochemical wastewater: a pilot study. Water Res 182, 116019, 1-9. https://doi.org/10.1016/j.watres.2020.116019.

13. Corda NC, & Kini MS (2018) A review on adsorption of cationic dyes using activated carbon. MATEC Web Conf (Vol. 144, p. 02022). EDP Sciences, 7-16. https://doi.org/10.1051/matecconf/201814402022.

14. González-García P (2018) Activated carbon from lignocellulosics precursors: A review of the synthesis methods, characterization techniques and applications. Renewable Sustainable Energy Rev 82, 1393-1414. https://doi.org/10.1016/j.rser.2017.04.117.

15. Saleem J, Shahid UB, Hijab M, Mackey H, & McKay G (2019) Production and applications of activated carbons as adsorbents from olive stones. Biomass Convers Biorefin 9(4), 775-802. https://doi.org/10.1007/s13399-019-00473-7.

16. Yang CY, Kao CL, & Hung PY (2022) Preparation of activated carbon from waste cation exchange resin and its application in wastewater treatment. Carbon Lett 32(2), 461-474. https://doi.org/10.1007/s42823-021-00275-w.

17. Moosavi S, Lai CW, Gan S, Zamiri G, Akbarzadeh Pivehzhani O, & Johan MR (2020) Application of efficient magnetic particles and activated carbon for dye removal from wastewater. ACS omega 5(33), 20684-20697. https://doi.org/10.1021/acsomega.0c01905.

18. Alam MM, Hossain MA, Hossain MD, Johir MAH, Hossen J, Rahman MS, & Ahmed MB (2020) The potentiality of rice husk-derived activated carbon: From synthesis to application. Processes 8(2), 203, 23-31. https://doi.org/10.3390/pr8020203.

19. Zhan Y, An X, Wang S, Sun M, & Zhou H (2020) Basil polysaccharides: A review on extraction, bi ACUMtivities and pharmacological applications. Bioorg Med Chem 28(1), 115179. 12-22. https://doi.org/10.1016/j.bmc.2019.115179.

20. Özsin G, Kılıç M, Apaydın-Varol E, & Pütün AE (2019) Chemically activated carbon production from agricultural waste of chickpea and its application for heavy metal adsorption: equilibrium, kinetic, and thermodynamic studies. Appl Water Sci 9(3), 1-14. https://doi.org/10.1007/s13201-019-0942-8.

21. Gan YX (2021) Activated Carbon from Biomass Sustainable Sources. C, 7(2), 39. https://doi.org/10.3390/c7020039.

22. Tomishima H, Luo K, & Mitchell AE (2021) The Almond (Prunus dulcis): Chemical Properties, Utilization, and Valorization of Coproducts. Annu Rev Food Sci Technol 13, 2-15. https://doi.org/10.1146/annurev-food-052720-111942.

23. Zhu M, Zhang L, Chen Y, You N, & Shen H (2022) Nanocomposites of Zirconia@ Activated Carbon Derived from Hazelnut Shell for Adsorption of Tetracyclines from Water. Environ Sci Technol, 223-306. https://doi.org/10.1039/D2EW00115B.

24. Liang Q, Liu Y, Chen M, Ma L, Yang B, Li L, & Liu Q (2020) Optimized preparation of activated carbon from coconut shell and municipal sludge. Mater Chem Phys 241, 122327. 1-28. https://doi.org/10.1016/j.matchemphys.2019.122327.

25. Agboola O, Okoli B, Sanni SE, Alaba PA, Popoola P, Sadiku ER, & Makhatha ME (2019) Synthesis of activated carbon from olive seeds: investigating the yield, energy efficiency, and dye removal capacity. SN Appl Sci 1(1), 1-10. https://doi.org/10.1007/s42452-018-0089-5.

26. Purnomo CW, Castello D, & Fiori L (2018) Granular activated carbon from grape seeds hydrothermal char. Appl Sci 8(3), 331-362. https://doi.org/10.3390/app8030331.

27. da Costa WK OC, Gavazza S, Duarte MMMB, Freitas SKB, de Paula NTG, & Paim APS (2021) Preparation of Activated Carbon from Sugarcane Bagasse and Removal of Color and Organic Matter from Real Textile Wastewater. Water Air Soil Pollut 232(9), 1-13. https://doi.org/10.1007/s11270-021-05306-w.

28. Menya E, Olupot PW, Storz H, Lubwama M, & Kiros Y (2018) Production and performance of activated carbon from rice husks for removal of natural organic matter from water: a review. Chem Eng Res Des 129, 271-296. https://doi.org/10.1016/j.cherd.2017.11.008.

29. Abbasi S, Foroutan R, Esmaeili H, & Esmaeilzadeh F (2019) Preparation of activated carbon from worn tires for removal of Cu (II), Ni (II) and Co (II) ions from synthetic wastewater. Desalin Water Treat 141, 269-278. https://doi.org/10.5004/dwt.2019.23569.

30. Togibasa O, Ansanay YO, Dahlan K, & Erari M (2021) Identification of surface functional group on activated carbon from waste sago. J Phys Theor Appl 5(1), 1-8. https://doi.org/10.20961/jphystheor-appl.v5i1.49885.

31. Alhogbi BG, Altaye, S, Bahaidarah E, & Zawrah MF (2021) Removal of anionic and cationic dyes from wastewater using activated carbon from palm tree fiber waste. Processes 9(3), 416-452. https://doi.org/10.3390/pr9030416.

32. Elkady M, Shokry H, & Hamad H (2020) New activated carbon from mine coal for adsorption of dye in simulated water or multiple heavy metals in real wastewater. Mater 13(11), 2498-2503. https://doi.org/10.3390/ma13112498.

33. Dobashi A, Maruyama J, Shen Y, Nandi M, & Uyama H (2018) Activated carbon monoliths derived from bacterial cellulose/polyacrylonitrile composite as new generation electrode materials in EDLC. Carbohydr Polym 200, 381-390. https://doi.org/10.1016/j.carbpol.2018.08.016.

34. Zhang W, Cheng H, Niu Q, Fu M, Huang H, & Ye D (2019) Microbial targeted degradation pretreatment: a novel appr ACUMh to preparation of activated carbon with specific hierarchical porous structures, high surface areas, and satisfactory toluene adsorption performance. Environ Sci Technol 53(13), 7632-7640. https://doi.org/10.1021/acs.est.9b01159.

35. Pang M, Huang Y, Meng F, Zhuang Y, Liu H, Du M, & Cai Y (2020) Application of bacterial cellulose in skin and bone tissue engineering. Eur Polym J 122, 109365. 2-22. https://doi.org/10.1016/j.eurpolymj.2019.109365.

36. Geravand SA, Khajavi R, Rahimi MK, Ghiyasvand MS, & Meftahi A (2022) Improving some structural and biological characteristics of bacterial cellulose by cross-linking. J Appl Polym Sci 139(18), 52056. 23-36. https://doi.org/10.1002/app.52056.

37. Ciecholewska-Juśko D, Żywicka A, Junka A, Drozd R, Sobolewski P, Migdał P, & Fijałkowski K (2021) Superabsorbent crosslinked bacterial cellulose biomaterials for chronic wound dressings. Carbohydr Polym 253, 117247.1-12. https://doi.org/10.1016/j.carbpol.2020.117247.

38. Khajavi, R., Meftahi, A., Alibakhshi, S., & Samih, L. (2014). Investigation of Microbial cellulose/Cotton/Silver nanobiocomposite as a modern wound dressing. Advanced Materials Research, 829, 616-621. https://doi.org/10.4028/www.scientific.net/AMR.829.616

39. Mirmohammadsadegh N, Shakoori M, Moghaddam HN, Farhadi R, Shahverdi AR, & Amin M (2021) Wound healing and anti-inflammatory effects of bacterial cellulose coated with Pistacia atlantica fruit oil. DARU J Pharm Sci 1-10. https://doi.org/10.1007/s40199-021-00405-9.

40. Eshgh, N. A., Meftahi, A., Khajavi, R., Aljabali, A. A., & Barhoum, A. (2022). Nanocelluloses for tissue engineering and biomedical scaffolds. In Handbook of nanocelluloses: classification, properties, fabrication, and emerging applications (pp. 1-36). Cham: Springer International Publishing. https://doi.org/10.1007/978-3-030-89621-8_43

41. Lee KY, Qian H, Tay FH, Blaker JJ, Kazarian SG, & Bismarck A (2013) Bacterial cellulose as source for activated nanosized carbon for electric double layer capacitors. J Mater Sci 48(1), 367-376. https://doi.org/10.1007/s10853-012-6754-y.

42. Khamkeaw A, Phanthang L, Jongsomjit B, & Phisalaphong M (2019) Activated carbon derived from bacterial cellulose and its use as catalyst support for ethanol conversion to ethylene. Catal Commun 129, 105750.1-7. https://doi.org/10.1016/j.catcom.2019.105750.

43. Khamkeaw A, Jongsomjit B, Robison J, & Phisalaphong M (2019) Activated carbon from bacterial cellulose as an effective adsorbent for removing dye from aqueous solution. Sep Sci Technol 54(14), 2180-2193. https://doi.org/10.1080/01496395.2018.1541906.

44. Khamkeaw A, Jongsomjit B, Yip AC, & Phisalaphong M (2022) Application of activated carbon derived from bacterial cellulose for mesoporous HZSM-5 catalyst synthesis and performances of catalyst in bioethanol dehydration. Biomass Bioenergy 160, 106440. 2-12. https://doi.org/10.1016/j.biombioe.2022.106440.

45. Koochaki CB, Khajavi R, Rashidi A, Mansouri N, & Yazdanshenas ME (2020) The effect of pre-swelling on the characteristics of obtained activated carbon from cigarette butts fibers. Biomass Convers Biorefin 10(2), 227-236. https://doi.org/10.1007/s13399-019-00429-x.

46. Meftahi A, Shahriari HR, Khajavi R, Rahimi MK, & Sharifian A (2020) Investigation on nano microbial cellulose/honey composite for medical application. Mater Res Express 7(8), 085003. 2-14. https://doi.org/10.1088/2053-1591/aba8de.

47. Chen H, Tang Z, Liu B, Chen W, Hu J, Chen Y, & Yang H (2021) The new insight about mechanism of the influence of K_2Co_3 on cellulose pyrolysis. Fuel 295, 120617. 1-9. https://doi.org/10.1016/j.fuel.2021.120617.

48. Zhu L, Zhao N, Tong L, & Lv Y (2018) Structural and adsorption characteristics of potassium carbonate activated biochar. RSC Adv 8(37), 21012-21019. https://doi.org/10.1039/C8RA03335H.

49. Luo, W., Guo, N., Wang, L., Jia, D., Xu, M., Zhang, S., ... & Cao, Y. (2023). Homogeneous activation induced by bacterial cellulose nanofibers to construct interconnected microporous carbons for enhanced capacitive storage. Journal of Colloid and Interface Science, 636, 33-41. https://doi.org/10.1016/j.jcis.2022.12.170.

50. Nishimura M, Iwasaki S, & Horio M (2009) The role of potassium carbonate on cellulose pyrolysis. J Taiwan Inst. Chem Eng 40(6), 630-637. https://doi.org/10.1016/j.jtice.2009.05.005.

51. Shu, Y., Bai, Q., Fu, G., Xiong, Q., Li, C., Ding, H., ... & Uyama, H. (2020). Hierarchical porous carbons from polysaccharides carboxymethyl cellulose, bacterial cellulose, and citric acid for supercapacitor. Carbohydrate Polymers, 227, 115346. 1-12. https://doi.org/10.1016/j.carbpol.2019.115346.

52. Gao Y, Yue Q, Gao B, & Li A (2020) Insight into activated carbon from different kinds of chemical activating agents: A review. Sci Total Environ 746, 141094. 1-19. https://doi.org/10.1016/j.scitotenv.2020.141094.

53. Heidarinejad Z, Dehghani MH, Heidari M, Javedan G, Ali I, & Sillanpää M (2020) Methods for preparation and activation of activated carbon: a review. Environ Chem Lett 18(2), 393-415. https://doi.org/10.1007/s10311-019-00955-0.

54. Yang S, Fecher S, Wang Q, Kühne M, & Smet JH (2022) Device level reversible potassium intercalation into bilayer graphene. 2D Mater 9(2), 025020.1-10. https://doi.org/10.1088/2053-1583/ac58a1.

55. Boongate C, & Phisalaphong M (2015) Activated carbons from bacterial cellulose by chemical activation with potassium hydroxide. Inter Conf Sci Tech (pp. 144-147). IEEE. 1-4. https://doi.org/10.1109/TICST.2015.7369351.

56. Zhao D, Guo Y, Wang G, & Mao X (2019) Characterizing nanoscale pores and its structure in coal: Experimental investigation. Energy Explor Exploit 37(4), 1320-1347. https://doi.org/10.1177/0144598719831397.

57. Chingombe P, Saha B, & Wakeman RJ (2005) Surface modification and 18haracterization of a coal-based activated carbon. Carbon 43(15), 3132-3143. https://doi.org/10.1016/j.carbon.2005.06.021.

58. Nguyen DT, Tran HN, Juang RS, Dat ND, Tomul F, Ivanets A, & Chao HP (2020) Adsorption process and mechanism of acetaminophen onto commercial activated carbon. J Environ Chem Eng Journal of 8(6), 104408. 23-36. https://doi.org/10.1016/j.jece.2020.104408.

59. Yagmur E, Gokce Y, Tekin S, Semerci NI, & Aktas Z (2020) Characteristics and comparison of activated carbons prepared from oleaster (Elaeagnus angustifolia L.) fruit using KOH and ZnCl2. Fuel 267, 117232. 1-8. https://doi.org/10.1016/j.fuel.2020.117232.

60. Saadatkhah N, Carillo Garcia A, Ackermann S, Leclerc P, Latifi M, Samih S, & Chaouki J (2020) Experimental methods in chemical engineering: thermogravimetric analysis—TGA. Can J Chem Eng 98(1), 34-43. https://doi.org/10.1002/cjce.23673.

61. Martínez-Sanz M, Lopez-Rubio A, & Lagaron JM (2011) Optimization of the nanofabrication by acid hydrolysis of bacterial cellulose nanowhiskers. Carbohydr Polym 85(1), 228-236. https://doi.org/10.1016/j.carbpol.2011.02.021.

62. Zhao, Q., Zhang, K., Zhu, S., Xu, H., Cao, D., Zhao, L., ... & Yin, W. (2019). Review on the electrical resistance/conductivity of carbon fiber reinforced polymer. Applied Sciences, 9(11), 2390. 1-25. https://doi.org/10.3390/app9112390.

63. Huang, Y. (2017). Electrical and thermal properties of activated carbon fibers. In Activated carbon fiber and textiles. Woodhead Publishing. 181-192. https://doi.org/10.1016/B978-0-08-100660-3.00007-9.

64. Adinaveen, T., Vijaya, J. J., & Kennedy, L. J. (2016). Comparative study of electrical conductivity on activated carbons prepared from various cellulose materials. Arabian Journal for Science and Engineering, 41, 55-65. https://doi.org/10.1007/s13369-014-1516-6.